International Journal of Heat and Technology
Vol. 43, No. 1, February, 2025, pp. 151-160
Journal homepage: http://iieta.org/journals/ijht

Energy Dissipation and Thermodynamic Characteristics Analysis During the Discharge Process of Hydraulic Gates

Xiang Zhou

Chongqing Water Resources and Electric Engineering College, Chongqing 402160, China

Corresponding Author Email: sljzls2024@163.com

https://doi.org/10.18280/ijht.430116

Received: 15 August 2024
Revised: 8 December 2024
Accepted: 21 December 2024
Available online: 28 February 2025

Keywords:
hydraulic gates, water discharge process, thermodynamic characteristics, energy dissipation, discharge entropy, thermal expansion coefficient, autogenous shrinkage deformation, creep deformation

ABSTRACT

Hydraulic gates play a central role in modern water resource management, where the thermodynamic characteristics and energy dissipation during the water discharge process significantly impact engineering efficiency and structural safety. Therefore, this study aims to in-depth investigate the thermodynamic characteristics and energy dissipation mechanisms during the water discharge process of hydraulic gates. The research background provides a review of the fundamental functions of hydraulic gates and the significance of the discharge process, highlighting the insufficient attention given in existing studies to energy dissipation and thermodynamic properties. Existing studies have primarily focused on macroscopic energy analyses, while the effects of microscopic entropy variations and material properties on discharge performance remain insufficiently explored. In this study, the concept of "discharge entropy" was introduced, and a comparative analysis between discharge entropy and thermodynamic entropy was conducted based on entropy theory and thermodynamic principles. A state variable solution method for discharge entropy was established, providing a novel theoretical framework for energy analysis in hydraulic disasters. Furthermore, the thermodynamic properties of the discharge process were examined in detail, including the thermal expansion coefficient, autogenous shrinkage deformation, and creep deformation of hydraulic gate materials. A computational model was proposed to offer more precise data support for the design and maintenance of hydraulic gates. These findings not only deepen the theoretical understanding of the thermodynamic behavior of hydraulic gates but also provide practical guidance for improving energy efficiency in engineering applications.

1. INTRODUCTION

Hydraulic gates play a crucial role in water resource management and hydraulic engineering design. They not only ensure effective river level control but also contribute significantly to flood prevention, irrigation, and hydroelectric power generation [1-4]. However, during the water discharge process, due to the complex interactions between fluid dynamics and thermodynamic effects, the energy transformation and dissipation patterns of hydraulic gate systems have become a focal point of interest for engineers and researchers [5-7]. A comprehensive understanding of the thermodynamic characteristics of this process is essential for enhancing the operational efficiency of hydraulic gates and extending their service life.

In recent years, with advancements in thermodynamics and fluid mechanics theories, increased attention has been directed toward investigating the energy conversion mechanisms and efficiency optimization of hydraulic gate discharge processes [8-11]. A quantitative analysis of energy dissipation during water discharge is not only beneficial for improving gate design and reducing operational costs but also plays a critical role in enhancing water resource utilization efficiency and mitigating water environmental pollution. Such analyses are essential for achieving sustainable hydraulic development strategies [12, 13].

Despite the insights gained from previous studies regarding energy conversion and dissipation during the water discharge process, certain limitations remain in the existing research methodologies [14-16]. In particular, a well-defined theoretical framework and quantitative analytical method integrating entropy theory with the hydraulic gate discharge process have yet to be established [17-22]. Moreover, the influence of hydraulic gate material properties on thermodynamic performance, including thermal expansion, autogenous shrinkage deformation, and creep deformation, has often been overlooked in current models, despite these factors being integral to energy dissipation analysis during discharge.

The primary objective of this study is to explore the application of entropy theory in the water discharge process of hydraulic gates and introduce the novel concept of "discharge entropy." A comparative analysis with conventional thermodynamic entropy was conducted, and a state variable solution method for discharge entropy was developed, offering a new theoretical perspective for entropy variation analysis in hydraulic disasters. Additionally, an in-depth investigation was conducted into the computation of thermodynamic performance parameters of hydraulic gates, including thermal expansion coefficients, autogenous shrinkage deformation, and creep deformation. The precise calculation of these thermodynamic parameters holds significant theoretical and practical value for optimizing hydraulic gate design and operational management. Through these two research components, this study aims to refine the analytical framework for the thermodynamic characteristics of hydraulic gate discharge processes and provide a scientific foundation for enhancing energy efficiency and sustainability in hydraulic engineering.

2. ENTROPY DYNAMICS IN GATE DISCHARGE

2.1 Entropy-gate discharge coupling mechanism

2.1.1 Flow entropy phenomena

During the water discharge process of hydraulic gates, the concept of entropy can be employed to describe the degree of disorder within the system, similar to the influence of temperature on entropy in thermodynamics. In this process, the entropy state of the system is not solely determined by the potential energy of the confined flow but is also influenced by the gate's capacity to regulate discharge. The observable entropy variation can be interpreted as the transformation of water from high potential energy to low potential energy, where energy dissipation occurs. This dissipation reflects an increase in the disorder of water flow as it passes through the gate, serving as a direct manifestation of entropy increase. Such dissipation is not merely an energy loss but also represents a potentially destructive force, as uncontrolled water discharge may lead to downstream flooding. By applying this concept to the discharge process of hydraulic gates, entropy can be redefined as a measure of kinetic energy loss and potential energy reduction as water flows through the gate. The design and operational control of the gate directly influences the magnitude of entropy. Hydraulic gates regulate flow velocity and discharge volume, thereby affecting entropy variation. From this perspective, entropy analysis of the discharge process in hydraulic gates not only facilitates a deeper understanding of flow dynamics and energy transformation mechanisms but also plays a critical role in enhancing discharge flow management efficiency and mitigating potential discharge-related risks.

2.1.2 Discharge entropy formulation

In the water discharge process of hydraulic gates, a new concept—discharge entropy—was introduced in this study. Discharge entropy is defined as a measure of the potential energy loss and the degree of disorder in water flow as it moves from upstream to downstream under the regulation of a hydraulic gate. Specifically, discharge entropy quantifies the increase in the unrestrained portion of water flow as it transitions from a higher potential energy state to a lower one through the gate. For instance, in a hydraulic gate system with a fixed capacity and control ability, variations in water volume and discharge duration result in different retention levels within the system. If the downstream water level is high, the upstream water flow experiences greater constraints, leading to an increase in its relative potential energy—representing the maximum energy state achievable without overflow. Consequently, the potential energy stored within the system increases, which in turn results in a higher value of discharge entropy.

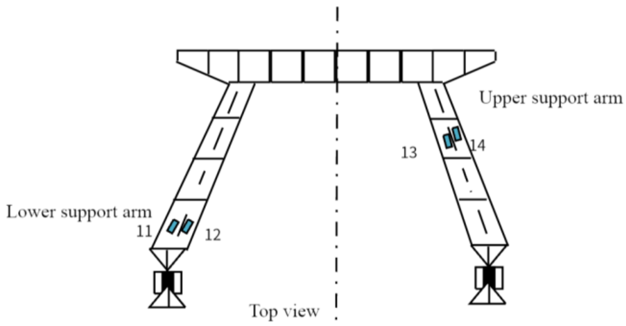

Figure 1. Schematic diagram of the hydraulic gate support structure and measurement point layout

The analysis of discharge entropy must take into account the following key aspects:

(1) Flow velocity and discharge volume control as water passes through the hydraulic gate, along with their effects on the potential energy of the flow.

(2) Energy dissipation of the water flow within the gate structure, including turbulence-induced dissipation and other forms of energy loss resulting from interactions between the water flow and the gate structure. Figure 1 illustrates the schematic diagram of the hydraulic gate support structure and the measurement point layout.

(3) The influence of gate operation on the entropy state of the water flow, as well as strategies for optimizing gate management to minimize discharge entropy and reduce the potential destructive force of the flow.

For hydraulic gates, the calculation of discharge entropy focuses on energy variations and losses occurring throughout the discharge process. During the water discharge process of hydraulic gates, discharge entropy can be estimated by monitoring and calculating the flow rate at the gate and its rate of change over time. Discharge entropy can be defined as the measure of increased system disorder due to variations in discharge volume and the corresponding energy transformation. Let ΔW_d denote the increase in discharge volume and N represents the overall discharge capacity of the hydraulic gate system. The discharge entropy ΔT_{du} for a given analytical interval u is expressed as follows:

$$\Delta T_{du} = \Delta W_{du} / N_s \tag{1}$$

2.1.3 Comparative analysis with thermodynamic entropy

In hydraulic engineering, discharge entropy can be regarded as an analogous concept for quantifying the degree of disorder of the water flow and energy dispersion within a system. Several similarities exist between discharge entropy and thermodynamic entropy:

(1) During the water discharge process of hydraulic gates, the mathematical expression of discharge entropy can be formulated in a manner similar to thermodynamic entropy. In this formulation, the initial conditions of the water flow, such as water level height and stored water volume, play a role analogous to the initial temperature in thermodynamics. Under the framework of discharge entropy, when an equal increase in water volume (ΔW_d) occurs, different initial water levels lead to varying degrees of disorder within the system. A higher initial water level indicates that the system initially possesses greater potential energy; therefore, the relative increase in disorder due to an equal increment in water volume is smaller, which can be attributed to a relatively small degree of disorder

caused by the newly added water compared to the initial state. This phenomenon is analogous to the principle in thermodynamics, where the introduction of an equal amount of heat into a system at a higher temperature result in a smaller change in entropy. Similarly, in the discharge process of hydraulic gates, if the system exhibits high flood regulation and storage capacity, the impact of an equal increase in water volume (ΔW_d) can be effectively absorbed and mitigated. Consequently, the relative variation in discharge entropy remains small. This is consistent with the behavior observed in thermodynamic systems with large heat capacity, where entropy variation is relatively lower when the same amount of heat is absorbed.

(2) In thermodynamics, dissipation refers to the phenomenon where energy is dispersed into a greater number of microscopic states during a natural process, leading to an increase in entropy. This process is irreversible, meaning that the total entropy of a system increases unidirectionally over time. A typical example of dissipation is the transfer of heat from a high-temperature region to a low-temperature region, during which the system loses energy order and experiences an increase in disorder. In this study, discharge entropy was introduced to characterize the dissipation of water flow energy and the increase in disorder during the discharge process of hydraulic gates. Under this framework, the increase in discharge entropy describes the transformation of potential energy into kinetic energy as water flows through the gate, followed by gradual dissipation due to factors such as friction and turbulence. This process is inherently irreversible, as once the water has passed through the gate, it cannot spontaneously return to its original high-potential energy state. The dissipation phenomenon in the discharge process of hydraulic gates can be understood in the following manner: the increase in discharge entropy during the process of hydraulic gate discharge describes the dissipation of energy when water flow is released from the gate. As the gate opens, water flows from a high-water-level region to a lower one, analogous to heat flowing from a high-temperature region to a low-temperature region. During this process, potential energy is converted into kinetic energy, and part of the energy is dissipated into the environment in the form of turbulence and impact forces exerted on the gate and riverbed, leading to an increase in the system's disorder. This energy transformation and dissipation process is irreversible, and as more water is released, the discharge entropy of the system continues to increase.

(3) In thermodynamics, entropy is a physical quantity that measures the degree of disorder within a system and can be used to assess the distribution of energy in irreversible processes. During an irreversible process, the total entropy of a system invariably tends to increase, reflecting the natural transition from an ordered state to a disordered state. This transition can be understood as the system's tendency to maximize its degrees of freedom within given constraints. That is, in accordance with natural laws, the system will spontaneously evolve toward a state of maximum entropy. In this study, discharge entropy was introduced as an evaluation metric for the irreversibility of the water discharge process and the distribution of energy. The increase in discharge entropy represents the transition of water flow from an ordered high-water-level state to a disordered low-water-level state, which inherently signifies energy dissipation during the discharge process. In the discharge process of hydraulic gates, energy is dissipated in the form of kinetic energy and turbulence, leading to an increase in the disorder within the system. Therefore, the increase in discharge entropy serves as a function for evaluating both energy dissipation and system state. By considering the practical conditions of hydraulic gate discharge, this concept can be further refined: during the water discharge process of hydraulic gates, discharge entropy describes the process by which water transitions from a high-potential-energy, ordered state to a low-potential-energy, disordered state as it passes through the gate. Similar to flood entropy, the increase in discharge entropy during the discharge process corresponds to the dissipation of kinetic and turbulent energy, thereby amplifying the disorder within the system. This increase in disorder reflects a reduction in the system's ability to constrain the water flow and an increase in the degrees of freedom of the flow. Notably, the variation in discharge entropy is independent of the specific discharge process but is solely related to the water level states before and after discharge. Consequently, the increase in discharge entropy can be regarded as an evaluation function for both energy and system state during the water discharge process of hydraulic gates.

2.2 Discharge entropy state variables

2.2.1 Energy input state function

In the case of hydraulic gate discharge, the primary energy forms involved are potential energy and kinetic energy, both of which vary with changes in water level and flow velocity. Therefore, the state function describing the input energy in the discharge process must not only account for variations in water volume but also include parameters such as the velocity and hydraulic head of the inflowing and outflowing water, as these factors are directly related to the energy state of the water flow. Specifically, the state function for input energy in the discharge process of hydraulic gates must consider the following factors: a) Difference in inflow and outflow water volume: Variations in water volume determine the increase or decrease in the stored water energy within the system. b) Difference in hydraulic head: The water level difference between the upstream and downstream directly influences the potential energy of the flow. c) Changes in flow velocity: Variations in water velocity affect the kinetic energy of the flow. d) Geographical parameters: The energy state of water at different positions within the discharge system may vary due to factors such as flow path, velocity distribution, and hydraulic structural characteristics. Similarly, energy dissipation during the discharge process must be considered in accordance with the second law of thermodynamics, as the irreversible nature of the water flow leads to energy dispersion. This is reflected through energy losses, turbulence generation, and other forms of dissipation. Assuming that in the u-th subregion of the system, at a given time in the hydraulic gate discharge process, the increase in water volume compared to the initial state is denoted as ΔW_d, and the water volume within the u-th subregion of the system at time S in the discharge process is denoted as W_{du}^{S}, while the water volume at the initial time 0 is denoted as W_{du}^{0}, with $W_{du}^{0}=W_{u0}$, the following definition equation is obtained:

$$\Delta W_{du} = \begin{cases} W_{du}^{S}, W_{du}^{S} \geq W_{du}^{0} \\ 0, W_{du}^{S} < W_{du}^{0} \end{cases} \tag{2}$$

For a specific hydraulic gate discharge process, the input energy of the water flow is determined by solving the governing equations of the water flow evolution process. Assuming that the reliability probability of the flood control structure corresponding to W_{ud}^{S} is denoted as o_e^u, and the discharge risk associated with the water flow W_{ud}^{S} is represented by Z_u, the number of computational subregions within the analyzed area is denoted as u, which is determined based on functional requirements and structural mechanics standards. Accordingly, the following equations are established:

$$\Delta W_{ud}^{O} = \Delta W_{ud} / o_e^u = W_{ud}^{S} / o_e^u \tag{3}$$

$$\Delta W_d = \sum_{u=1}^{v} \Delta W_{ud}^{o} \tag{4}$$

It can be observed that as W_{ud}^{S} increases, the value of o_e^u decreases, leading to a reduction in the overall discharge capacity of the hydraulic gate system.

2.2.2 Discharge capacity state function

Figure 2 illustrates the schematic layout of the gate leaf, main beams, and longitudinal beams in a hydraulic gate, along with the arrangement of measurement points. The comprehensive discharge capacity of a hydraulic gate is a complex concept, as it depends on the mechanical properties and spatial positioning of various structural components within the system. In the water discharge process of hydraulic gates, the computation of the state function for comprehensive discharge capacity must take into account the following factors to ensure its applicability to practical discharge scenarios: a) Discharge capacity: This metric quantifies the volume of water that can be safely released by the hydraulic gate and is influenced by both gate design and operational conditions. b) Hydraulic head and flow velocity: The hydraulic head (i.e., water level difference) and flow velocity determine the potential and kinetic energy of the water, both of which are fundamental to energy conversion during the discharge process. c) Structural reliability: The integrity of the gate structure directly affects its discharge performance. Therefore, structural reliability under varying discharge conditions must be evaluated. For the computation of the state function representing the comprehensive discharge capacity of hydraulic gates, the reliability of relevant structures within the system and the potential impact zones affecting the discharge process must be comprehensively considered. Accordingly, the following equation is established:

$$\begin{aligned} &\textit{Discharge volume}\left(W_{e0}^{u}\right) = \\ &\textit{Actual discharge water volume}\left(W_{u0}\right) \\ &*\textit{Structural reliability probability}\left(o_{e0}^{u}\right) \end{aligned} \tag{5}$$

The formula for calculating the comprehensive discharge capacity of hydraulic gates is given as follows:

$$N = \sum_{u=1}^{v} W_{e0}^{u} \tag{6}$$

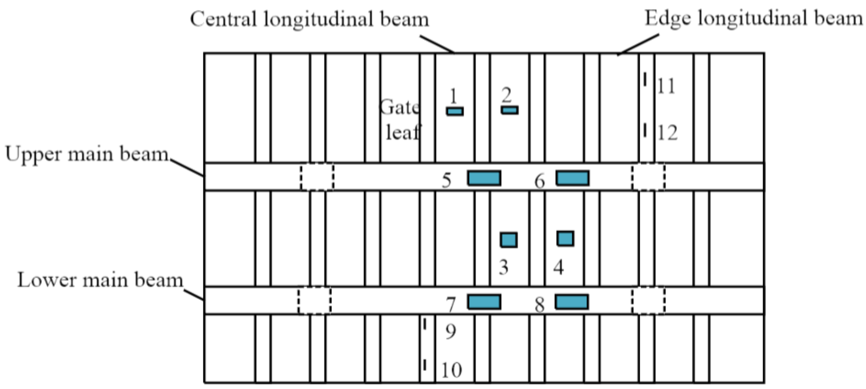

Figure 2. Schematic diagram of the layout of the gate leaf, main beams, and longitudinal beams in a hydraulic gate, along with measurement point locations

2.2.3 Entropy quantification method

Discharge entropy describes the uncertainty and disorder of the system state during the discharge process. It is closely related to the potential losses caused by discharge, energy dissipation, and the efficiency of discharge control. The uncertainty within the system during discharge is directly influenced by the capacity to regulate water volume and the efficiency of discharge operations. Therefore, the calculation of discharge entropy must account for the following key factors:

(1) Water volume regulation coefficient: This parameter quantifies the system's ability to control flow rate and is denoted as β_{u0}. It is influenced by the design of the discharge outlet, operational strategies, and control mechanisms.

(2) Regional impact: The area affected by the subregion controlled by the gate, along with economic indicators related to water flow hazards, must be considered, as they indicate the potential economic losses associated with the discharge process.

(3) Energy dissipation: Energy loss during the discharge process, including hydraulic losses and energy dissipation due to friction and turbulence, affects discharge efficiency and the entropy state of the system.

Assuming that the area controlled by the u-th structural unit of the system is represented by X_{u0}, and the average system discharge efficiency indicator per unit area within this range is denoted as Z_{u0}, then $\Delta T_{su}=\Delta T_{su}/N_u$ leads to $\Delta T_d=\sum^{v}_{u=1}\Delta T_{su}=\sum^{v}_{u=1}\Delta T_{su}/N_u$.

$$\beta_{u0} = \frac{X_{u0} Z_{u0}}{\sum_{u=1}^{v} X_{u0} Z_{u0}} \tag{7}$$

$$
\begin{aligned}
\Delta T_d &= \sum_{u=1}^{v} \Delta W_{du}^{O} \beta_{u0} \big/ W_{u0}^{u} \\
&= \sum_{u=1}^{v} W_{du}^{S} * X_{u0} Z_{u0} \Big/ \left[o_e^u \left(u \sum_{i=1}^{v} X_{u0} Z_{u0} \right) W_{u0} o_{e0}^{u} \right] \\
&= \sum_{u=1}^{v} \left(\frac{W_{du}^{S}}{W_{u0}} * \frac{X_{u0} Z_{u0}}{o_e^u \left(\sum_{u=1}^{v} X_{u0} Z_{u0} \right) o_{e0}^{u}} \right) \\
&= \sum_{u=1}^{v} \left(\frac{W_{du}^{S}}{W_{u0}} * \frac{X_{u0} Z_{u0}}{\sum_{u=1}^{v} X_{u0} Z_{u0}} * \frac{1}{o_e^u o_{e0}^{u}} \right)
\end{aligned}
\tag{8}
$$

From the expression of the discharge entropy function, it can be observed that three primary factors influence the discharge entropy value:

(1) The influence of hydraulic factors in the hydraulic gate discharge process on discharge entropy, represented by W_{du}^{S} / W_{u0} . This term primarily reflects the relationship between the actual water discharge volume W_{du}^{S} and the maximum water volume W_{u0} that the system structure can safely accommodate. The greater the difference between W_{du}^{S} and W_{u0}, the higher the discharge entropy value.

(2) The influence of flood-induced economic losses on discharge entropy, represented by $X_{u0}Z_{u0}/\sum^{v}_{u=1}X_{u0}Z_{u0}$.

(3) The function of structural failure probability $1/(1-o_d^u)(1-o_0^{ud})$, where the reliability probability is denoted as o_e, and the failure probability is denoted as o_d. In addition, o_d^u and o_0^{ud} represent the structural failure probability under the initial water flow analysis state and under the water flow analysis state at a specific moment during the hydraulic gate discharge process, respectively. This effect is reflected by $1/o_e^u o_{e0}^u$, where o_e and o_d sum to 1. Therefore, the expression $1/(1-o_d^u)(1-o_0^{ud})$ can also be interpreted in this context.

3. THERMODYNAMIC PERFORMANCE CHARACTERIZATION

During the water discharge process of hydraulic gates, thermodynamic performance parameters serve as critical indicators for evaluating the response of structural materials to temperature variations. The following definitions pertain to the early-stage thermal expansion coefficient, autogenous shrinkage deformation, and creep deformation, incorporating both the thermodynamic and mechanical behaviors that hydraulic gates may experience during discharge.

(1) The early-stage thermal expansion coefficient characterizes the volumetric expansion or contraction of a material due to temperature fluctuations during its initial curing phase. This parameter is particularly significant for hydraulic gates, as materials such as concrete may develop cracks due to temperature differentials during this stage, potentially compromising the structural integrity and discharge functionality of the gate. The early-stage thermal expansion coefficient defines the rate of unit length change per unit temperature variation, serving as a key parameter for predicting and mitigating early-stage material stress induced by temperature fluctuations in the discharge process. Assuming that the stabilized value of the thermal expansion coefficient is denoted as $\beta_S(s_r)$ and the parameters to be fitted are represented by l and v, the calculation formula is given as follows:

$$
\beta_S\left(s_r\right) = \beta_t \bullet \left(1 + l s_r^{v}\right) \tag{9}
$$

(2) Autogenous shrinkage refers to the volumetric reduction caused by internal moisture evaporation in the absence of external loads or temperature gradients. During the discharge process of hydraulic gates, autogenous shrinkage deformation is a crucial factor affecting long-term structural stability. Due to continuous water flow and variations in environmental humidity, the gate materials undergo autogenous shrinkage deformation, which may compromise structural stability, thereby impacting discharge efficiency and safety. Assuming that the autogenous shrinkage strain of panel concrete at an equivalent age s_r is represented by $\gamma_X(s_r)$, and the final stabilized autogenous shrinkage value is denoted as γ_0, with the coefficients to be fitted represented by ω and λ, the corresponding calculation formula is expressed as follows:

$$
\gamma_X\left(s_r\right) = \gamma_0 \bullet \exp\left[-\left(\frac{\omega}{s_r} \right)^{\lambda} \right] \tag{10}
$$

(3) Creep deformation refers to the slow and continuous deformation of a material under sustained loading over an extended period. In hydraulic gate structures, creep deformation is essential for assessing and maintaining the operational lifespan of the gate. Due to prolonged exposure to water pressure, environmental temperature fluctuations, and humidity variations, hydraulic gate materials exhibit creep effects. This deformation tends to accumulate over time, potentially affecting the performance and safety of the discharge structure. Therefore, the prediction and control of creep deformation are critical aspects of hydraulic gate maintenance and management. Assuming that the age of gate concrete is denoted as π, the sustained loading duration is expressed as s-π, and the parameters to be fitted are represented by x, y, z, f, r, d, h, and g, the calculation formula is given as follows:

$$
\begin{aligned}
Z\left(s,\pi\right) &= \left(x + y\pi^{-z}\right)\left[1 - r^{-f(s-\pi)}\right] \\
&+ \left(r + d\pi^{-h}\right)\left[1 - r^{-gs(t-\pi)}\right]
\end{aligned}
\tag{11}
$$

4. EXPERIMENTAL RESULTS AND ANALYSIS

Table 1 presents a comprehensive set of hydraulic gate simulation parameters, which are utilized to model the operation of an arc-shaped gate with inclined support arms. The gate dimensions, measuring 18 meters in width and 11 meters in height, align with the design water retention level of 125.0 meters, ensuring adequate water flow capacity. The hoist system, comprising 2×2500 kN hydraulic hoists, is responsible for controlling gate opening and closing. Its force configuration is coordinated with the gate dimensions and the design head of 11.4 meters, ensuring stable operation. The pivot center distance of 18.5 meters and the dual hoisting point configuration are adapted to the structural design of the gate, facilitating stable and controlled movement. Furthermore, the full open-to-full close rotation angle of approximately 65° and the maximum transport unit weight of approximately 42 tons reflect the practical operational parameters and feasibility of the engineering implementation. As shown in Table 2, the thermodynamic performance parameters of the experimental specimens were meticulously selected to ensure the effectiveness and reliability of the hydraulic gate during actual operation. The selection of thermal expansion coefficient, thermal conductivity, and specific heat capacity accounts for the material behavior under temperature variations and heat transfer processes. Meanwhile, elastic modulus, Poisson's ratio, tensile strength, and yield strength ensure structural stability under mechanical loading conditions. These parameters not only reflect the intrinsic physical properties of the structural materials but are also tailored to meet design requirements and operational conditions.

Table 3 presents the structural strength simulation analysis results for various components of the hydraulic gate. The principal stress and maximum shear stress for each component remain within their respective adjusted allowable stress limits. The principal stress in the gate leaf is 200.36 MPa, significantly lower than its adjusted allowable stress of 345.21 MPa. Similarly, the maximum shear stress of the gate leaf does not exceed its allowable value. Other components, including the main beam, support arm, and longitudinal arm, also exhibit simulated stress values below their respective adjusted allowable stress limits. These results clearly demonstrate that the structural strength of the hydraulic gate satisfies engineering safety and operational requirements, thereby verifying the structural reliability and safety. The accurate calculation of thermodynamic performance parameters is crucial for ensuring the stability and durability of the gate under actual operating conditions. The integration of these thermodynamic parameters into the discharge entropy concept and state variable computation not only provides a novel theoretical perspective for entropy variation analysis in hydraulic disasters but also offers robust theoretical support for the design and operational management of hydraulic gates, reinforcing the practicality and forward-looking nature of the proposed methodology.

Table 1. Hydraulic gate simulation parameter specifications

Parameter	Specification
Gate type	Arc-shaped gate with inclined support arms
Hoist Type	2×2500 kN hydraulic hoist
Orifice dimensions (width × height)	18 m×11 m
Design water retention level	125.0 m (normal storage level)
Bottom sill elevation	114.00 m
Design head	11.4 m
Operating head	11 m
Pivot center distance	18.5 m
Hoisting point configuration	Dual hoisting points
Maximum transport unit weight	Approximately 42 t
Full open-to-full close rotation angle	Approximately 65°

Table 2. Thermodynamic parameters of hydraulic gate structural materials

Thermodynamic Parameter	Value	Unit
Density	7750	kg/m³
Thermal expansion coefficient	1.35×10^{-3}	/°C
Elastic modulus	180	GPa
Poisson's ratio	0.28	--
Thermal conductivity	62.4	W/m·°C
Specific heat capacity	425	J/kg·°C
Tensile strength	489	MPa
Yield strength	346	MPa

Table 3. Structural strength simulation analysis results of the hydraulic gate

	Component	Maximum Simulation Result (MPa)	Adjusted Allowable Stress (MPa)	Analysis Conclusion
Gate leaf	Principal stress	200.36	345.21	Meets design specifications
	Maximum shear stress	112.23	127.48	Meets design specifications
Main beam	Principal stress	157.23	223.69	Meets design specifications
	Maximum shear stress	87.36	127.89	Meets design specifications
Support arm	Principal stress	135.26	223.15	Meets design specifications
	Maximum shear stress	78.16	124.59	Meets design specifications
Longitudinal arm	Principal stress	137.96	223.59	Meets design specifications
	Maximum shear stress	78.23	127.89	Meets design specifications

Table 4. Temperature and stress calculation results of the hydraulic gate at selected measurement points during the water discharge process

Measurement Point	Temperature or Stress Condition	Strongly Constrained Region		Weakly Constrained Region		Gate Leaf	Main Beam	Support Arm	Longitudinal Arm
		Region III	Region IV	Region III	Region V				
1	Maximum temperature (°C)	30.2	28.9	38.2	35.2	43.2	45.7	43.2	41.2
	Maximum tensile stress (MPa)	1.2	1.1	0.9	1.7	1.8	2.2	3.5	1.5
2	Maximum temperature (°C)	30.2	28.9	38.2	35.2	43.2	45.7	43.2	41.2
	Maximum tensile stress (MPa)	1.2	1.1	1.0	1.7	1.8	2.2	3.5	1.5
3	Maximum temperature (°C)	30.2	28.9	38.2	35.2	43.2	45.7	43.2	41.2
	Maximum tensile stress (MPa)	1.2	1.1	1.0	1.7	1.8	2.2	3.5	1.5
4	Maximum temperature (°C)	30.2	28.9	38.2	35.2	43.2	45.7	43.2	41.2
	Maximum tensile stress (MPa)	1.2	1.1	1.0	1.7	1.8	2.5	4.8	1.5

Based on the data presented in Table 4, variations in temperature and stress distribution across different regions of the hydraulic gate and the constrained regions during the discharge process can be observed. The temperature measurements indicate that the weakly constrained region exhibits relatively lower temperatures (ranging from 28.9℃ to 30.2℃), whereas the gate leaf and longitudinal arm experience significantly higher temperatures (reaching 41.2℃ to 45.7℃). This suggests that these components are more susceptible to solar radiation or other heat sources. Stress analysis results reveal that the gate leaf and longitudinal arm experience relatively high maximum tensile stress, particularly at measurement point 4, where the tensile stress in the longitudinal arm reaches 4.8 MPa. This increase in stress is attributed to material expansion caused by temperature elevation. Although the recorded stress values remain within the material's permissible stress limits, continuous thermal cycling and mechanical loading could contribute to fatigue and cumulative structural damage over time. The proposed thermodynamic characteristics analysis and the concept of discharge entropy are effectively reflected in the experimental results. Through real-time monitoring of temperature and stress, variations in thermal stress throughout the discharge process can be observed, validating the applicability of the discharge entropy state variable computation method.

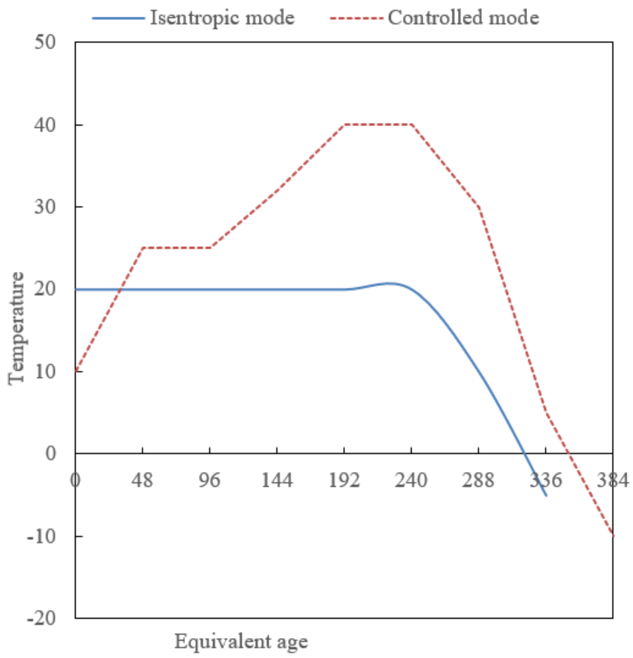

a) Temperature

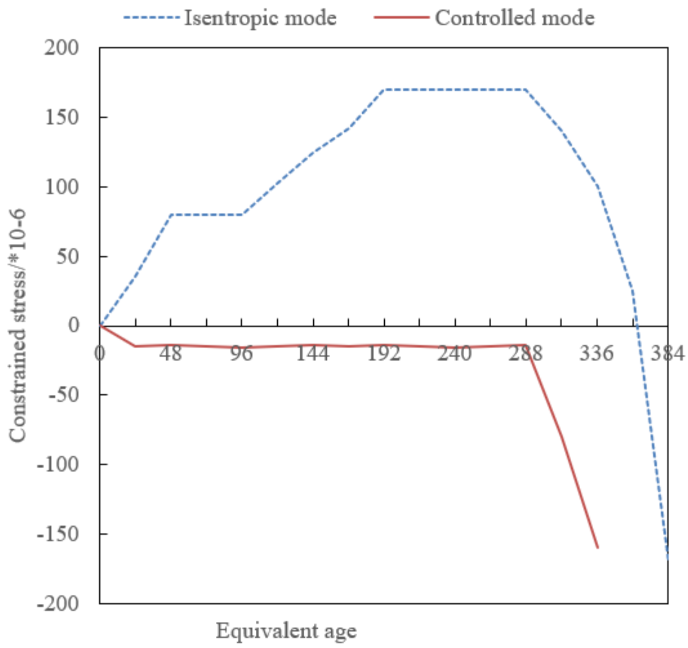

b) Free strain

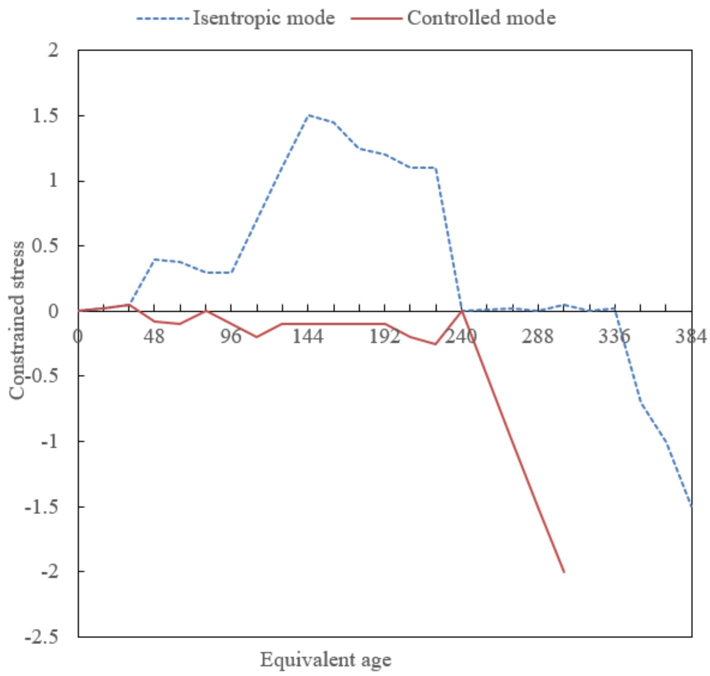

c) Constrained stress

Figure 3. Development curves of temperature, free strain, and constrained stress in the hydraulic gate

Figure 3 presents the development curves of temperature, free strain, and constrained stress in the hydraulic gate under different equivalent ages. The temperature curve indicates that under the isentropic mode, the temperature remains stable, whereas under the controlled mode, the temperature initially increases and then decreases with equivalent age. This suggests that the controlled mode effectively regulates the temperature of the gate, allowing it to adapt to external environmental variations. The free strain data reveal that under the isentropic mode, free strain increases over time, exhibiting the creep characteristics of the material under sustained loading. In contrast, under the controlled mode, free strain exhibits greater variation, particularly in later stages, where a more pronounced negative strain is observed, indicating a more proactive strain control strategy. For constrained stress, the results show that under the isentropic mode, stress gradually increases and stabilizes, whereas under the controlled mode, constrained stress initially exhibits negative values before transitioning to positive values, reflecting the significant impact of external control strategies on the stress state. The experimental data validate the effectiveness of both the isentropic mode and the controlled mode in regulating the thermodynamic behavior of hydraulic gates. The isentropic mode, by maintaining a constant temperature and reducing energy dissipation compared to conventional thermodynamic entropy, enhances structural stability. Meanwhile, the controlled mode, by actively adjusting temperature and strain, enables greater adaptability to environmental and load variations, thereby optimizing structural performance.

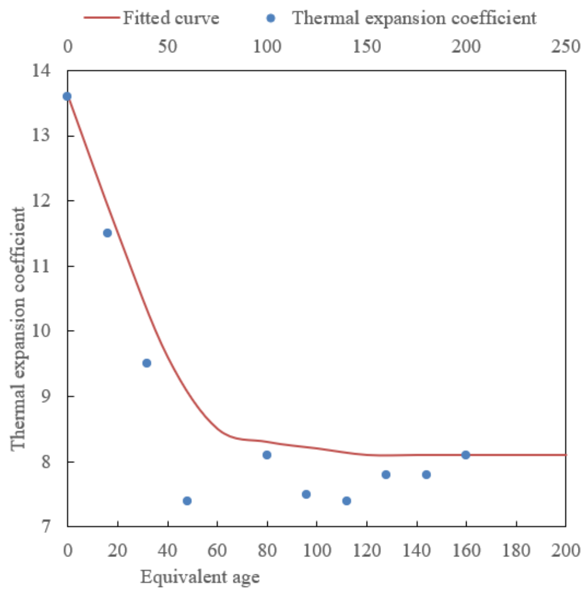

Figure 4. Fitted curve of the thermal expansion coefficient of the hydraulic gate

The data presented in Figure 4 illustrate the variation of the thermal expansion coefficient of the hydraulic gate over different equivalent ages. During the initial phase, the thermal expansion coefficient decreases from 13.6 to 7.4, indicating a gradual reduction in the material's thermal expansion capacity over time. This phenomenon is associated with the internal structural adjustment and rearrangement of the material as it ages. After reaching an equivalent age of 80, the thermal expansion coefficient exhibits a slight recovery, eventually stabilizing around 8.1. The fitted curve reflects the overall trend, showing a sharp initial decline followed by stabilization. This trend suggests that in later stages, the thermal expansion behavior of the gate material becomes more consistent, which is critical for ensuring long-term operational stability. Through the experimental data on the thermal expansion coefficient and its fitted curve, the variation patterns of thermodynamic properties at different material ages were validated. These findings further confirm the effectiveness of the discharge entropy theory in analyzing and predicting the thermodynamic performance of hydraulic gates. The variation of the thermal expansion coefficient is directly linked to material stability under temperature fluctuations and energy dissipation, while maintaining stable thermal expansion properties is essential for reducing thermal stress concentration and preventing material fatigue and fracture.

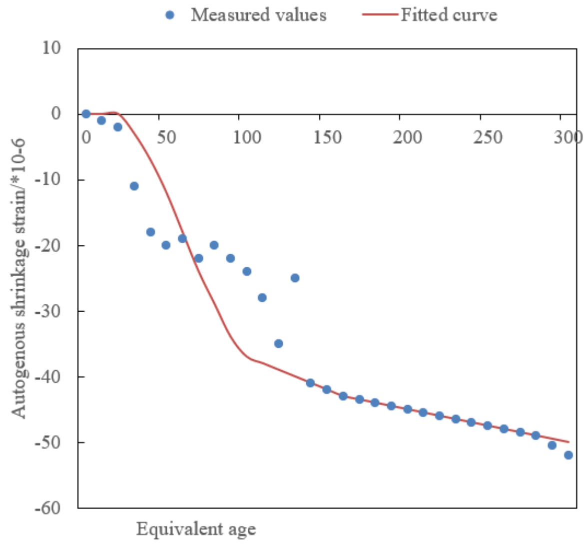

Figure 5. Measured and predicted early-age autogenous shrinkage deformation of the hydraulic gate

Figure 5 presents the measured values of early-age autogenous shrinkage deformation of the hydraulic gate under different equivalent ages, along with the predicted curve obtained through data fitting. The measured values indicate that autogenous shrinkage deformation increases slowly during the initial stage (equivalent age from 0 to 50 days), followed by an accelerated growth phase (50 to 150 days), reaching a pronounced peak at 150 days. Subsequently, the deformation growth rate gradually slows, though an overall increasing trend persists, approaching -52 at 300 days. The fitted curve depicts a smoother growth trend for autogenous shrinkage deformation. However, compared to the measured values, the fitted curve underestimates the rate of deformation increase during the first 150 days. Additionally, fluctuations in the measured values at certain equivalent ages are observed, which can be attributed to variations in material composition, environmental factors, or construction conditions. A comparison between the measured autogenous shrinkage deformation and the fitted curve reveals that the overall trend of the fitted curve effectively captures the development pattern of autogenous shrinkage deformation, despite some discrepancies. These deviations are primarily due to the complexities of real-world engineering conditions, including material heterogeneity, temperature fluctuations, and humidity variations. Nonetheless, the fitted curve still provides a valuable reference for understanding and predicting early-age autogenous shrinkage deformation.

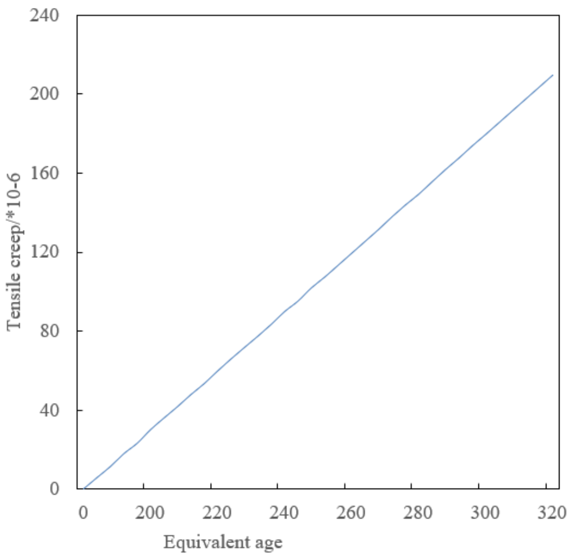

a) Tensile creep curve

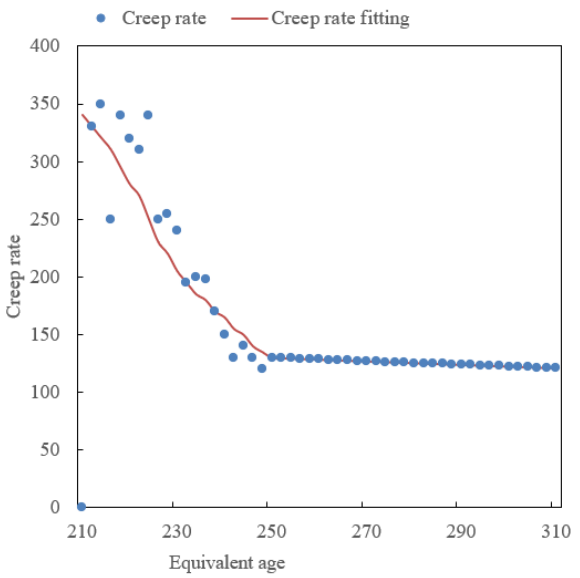

b) Fitted creep rate curve

Figure 6. Creep curve and fitted creep rate curve of the hydraulic gate

Based on the data presented in Figure 6, the creep curve of the hydraulic gate reveals that tensile creep values increase progressively with equivalent age, rising from 0 at day 0 to 203.5 at day 300. The data indicate that creep growth is relatively slow in the early stages but accelerates over time, particularly between 200 and 300 days, where a significant increase in creep is observed. Meanwhile, the fitted curve of the creep rate illustrates a stabilization trend over time, decreasing from 340 at day 210 to 121 at day 310, indicating a gradual decline in the creep rate. Although deviations between the fitted curve and the measured values exist, the overall trend is well captured, reflecting the evolution of material creep properties over time. The behavior revealed by both the creep curve and the fitted creep rate curve demonstrates the time-dependent thermodynamic characteristics of the hydraulic gate materials. This creep phenomenon is directly correlated with internal energy dissipation within the material. As the material ages, microscopic structural reorganization occurs, leading to progressive energy dissipation. This energy transformation is consistent with the second law of thermodynamics, wherein entropy increases as the system undergoes spontaneous processes. Through the introduction of the discharge entropy concept, integrated with the traditional theory of thermodynamic entropy, a novel state variable computation method was successfully developed, offering a new analytical tool for entropy variation in hydraulic disasters. The findings indicate that this study not only presents theoretical innovations but also demonstrates clear practical significance in predicting material performance changes, guiding hydraulic gate design, and optimizing operational management.

5. CONCLUSION

Through a series of experimental investigations and theoretical analyses, the thermodynamic properties and creep behavior of hydraulic gates during the discharge process were extensively studied. The concept of discharge entropy was successfully introduced and defined, providing an innovative theoretical perspective for analyzing entropy variation in hydraulic flow disasters. By conducting a comprehensive analysis of structural strength, temperature and stress distribution, thermal expansion coefficient, autogenous shrinkage, and creep characteristics, the entropy variation phenomenon of materials during the discharge process was elucidated, and a complete computational framework for thermodynamic parameters was established. These methodologies are crucial for understanding and predicting the performance of hydraulic gates in actual operating environments. The findings demonstrate that precise calculations of thermodynamic performance parameters enable the optimization of hydraulic gate design, enhancing adaptability and durability under complex working conditions.

The significance of this study lies in both its theoretical innovation and practical implications, providing a novel tool for design and evaluation in the field of hydraulic engineering. However, certain limitations exist in this study. For instance, experimental conditions and material properties may differ from actual extreme working conditions. Future research should focus on validating and extending the proposed theoretical framework across a broader range of operating conditions and material types. Additionally, further refinement and expansion of the discharge entropy concept, particularly in its application to early warning systems for hydraulic disasters, require extensive experimental data and in-depth theoretical exploration. Future studies should also prioritize the long-term creep behavior of hydraulic gates and its implications for structural safety, as well as explore the potential applications of entropy theory in other hydraulic engineering structures.

ACKNOWLEDGMENT

This paper was supported by Chongqing Special and Key Project for Technology Innovation and Application Development (Grant No.: CSTB2022TIAD-KPX0132).

REFERENCES

[1] Cai, Y., Xiang, Y., Sheng, J., Meng, Y. (2023). Deep-water detection, monitoring, early warning and treatment

of emergencies of major water conservancy projects: A review. Chinese Journal of Geotechnical Engineering, 45(3): 441-458. https://doi.org/10.11779/CJGE20221480

[2] Qasim, R.M., Abdulhussein, I.A., Naeem, S.M., Maatooq, Q.A. (2024). Experimental investigation of emerged dike influence on combined discharge structures in open channel flow. Mathematical Modelling of Engineering Problems, 11(2): 367-374. https://doi.org/10.18280/mmep.110208

[3] Zhao, P., Zhao, Y., Li, S., Yang, J., Xu, J., Li, L., Zhao, X. (2022). Numerical simulation of the hydraulic performance of spillway of Goushuipo reservoir. International Journal of Heat & Technology, 40(3): 729-736. https://doi.org/10.18280/ijht.400310

[4] Zhang, Y., Mao, Y., Huang, H., Lan, L., Lu, N. (2021). Water quality simulation and improvement under the combined scheduling of sluice gates and pumps in the Lixia River area. In 2021 7th International Conference on Hydraulic and Civil Engineering & Smart Water Conservancy and Intelligent Disaster Reduction Forum (ICHCE & SWIDR), Nanjing, China, pp. 1801-1805. https://doi.org/10.1109/ICHCESWIDR54323.2021.9656278

[5] Yue, X., Xu, Y., Zhou, X., Zhang, X., Linghu, Y., Wang, X., Chen, H. (2023). Performance in the discharge process of a novel zeolite-water adsorption thermal energy storage system. Journal of Thermal Science, 32(4): 1626-1634. https://doi.org/10.1007/s11630-023-1727-9

[6] Deshmukh, A., Foo, Z.H., Stetson, C., Lee, H., Orme, C.J., Wilson, A.D., Lienhard, J.H. (2022). Thermodynamics of solvent-driven water extraction from hypersaline brines using dimethyl ether. Chemical Engineering Journal, 434: 134391. https://doi.org/10.1016/j.cej.2021.134391

[7] Zhang, L., Fu, Q., Ding, S., Liu, K., Li, K., Zhang, X., Pei, Y. (2023). Thermodynamic characteristics of the hot-temperature cavity generated by the spark discharge in saline water. International Journal of Heat and Mass Transfer, 215: 124498. https://doi.org/10.1016/j.ijheatmasstransfer.2023.124498

[8] Zhang, Y., Zhao, H., Fu, C., Tie, Y., Li, H. (2022). Automatic identification of the operational modal parameters for hydraulic gates under flow release excitation. Transactions of the Chinese Society of Agricultural Engineering (Transactions of the CSAE), 38(20): 59-66. https://doi.org/10.11975/j.issn.1002-6819.2022.20.007

[9] Rakib, Z., Zeng, J., Ansar, M., Hajimirzaie, S. (2022). Energy dissipation design of low-head hydraulic structures using computational fluid dynamics model. In World Environmental and Water Resources Congress 2022, pp. 297-310. https://doi.org/10.1061/9780784484258.028

[10] Liu, S.H., Liao, T.T., Luo, Q.S. (2015). Numerical simulation of turbulent flow behind sluice gate under submerged discharge conditions. Journal of Hydrodynamics, 27(2): 257-263. https://doi.org/10.1016/S1001-6058(15)60480-2

[11] Dezert, T., Ravindra, G.H.R., Sigtryggsdóttir, F.G. (2022). Placed riprap deformation related to axial load at toe support: Physical modelling. Water, 14(10): 1581. https://doi.org/10.3390/w14101581

[12] Chen, C., Zhang, S., Li, B. (2024). Realizing high energy density and discharge energy density in high hardness Ba1. 938Bi0. 375Nb5O15-based glass ceramics. Ceramics International, 50(1): 650-659. https://doi.org/10.1016/j.ceramint.2023.10.143

[13] Huang, Y., Liu, Y., Yan, N., Zhao, X., Zhao, X., Li, Y., Jia, Z. (2023). Research on new ceramic debinding technology with low energy consumption via dielectric barrier discharge. Physica Scripta, 98(4): 045904. https://doi.org/10.1088/1402-4896/acc2f6

[14] Deng, C., Liu, Z., Pan, H., Qiu, M. (2023). Improvement of part straightness accuracy by controlling discharge energy in WEDM. The International Journal of Advanced Manufacturing Technology, 126(9): 4685-4694. https://doi.org/10.1007/s00170-023-11462-6

[15] Zhang, Y., Yang, X., Gao, Q., Wang, J., Zhao, W. (2023). Mechanism analysis of discharge energy in the electrostatic-field-induced electrolyte jet Micro-EDM. Micromachines, 14(10): 1919. https://doi.org/10.3390/mi14101919

[16] Xu, Z., Guo, Y., Wu, S. (2023). Analysis of spark discharge energy conversion in igniters. High Voltage Engineering, 49(8): 3315-3323. https://doi.org/10.13336/j.1003-6520.hve.20221677

[17] Windarto, C., Lim, O. (2023). Spark discharge energy effect on in-cylinder characteristics performance of rapid compression and expansion machine with spark ignition direct injection strategy. Fuel, 337: 127165. https://doi.org/10.1016/j.fuel.2022.127165

[18] Ceritbinmez, F., Kanca, E., Yünlü, L., Patel, K., Akhtar, M. A., Mukherjee, S., Günen, A. (2023). Wire electric discharge machining and its effect on the surface finish of HfNbTaTiZr refractory high-entropy alloy. The International Journal of Advanced Manufacturing Technology, 125(3): 1419-1427. https://doi.org/10.1007/s00170-022-10797-w

[19] Omori, Y., Yoshimura, H., Fujita, I., Watanabe, K. (2024). Flood discharge measurement by STIV coupled with maximum entropy method using parameter estimation by numerical analysis. KSCE Journal of Civil Engineering, 28(3): 1122-1131. https://doi.org/10.1007/s12205-024-1458-9

[20] Feng, T., Liu, C.S., Xu, A., Wang, C.H., Wang, F.M., Liu, X., Su, S.T. (2023). Research on transformer partial discharge feature extraction based on empirical wavelet transform and multiscale permutation entropy. Journal of Physics: Conference Series, 2492(1): 012010. https://doi.org/10.1088/1742-6596/2492/1/012010

[21] Ahamed, N., Kundu, S. (2023). Fractional entropy-based modeling of suspended concentration distribution of type I and type II and sediment discharge in pipe and open-channel turbulent flows. Zeitschrift für angewandte Mathematik und Physik, 74(3): 101. https://doi.org/10.1007/s00033-023-01988-w

[22] Niu, S., Sun, K., Mu, R., Wang, Y., Yang, Z. (2023). Facile preparation of multiscale high-entropy carbide particles utilizing pulse discharge: Phase and microstructure evolution. Advanced Engineering Materials, 25(13): 2300236. https://doi.org/10.1002/adem.202300236